

Response of Ocean Circulation to Variable Wind Forcing

A.E. Kiss^{1,2} and C. Ménesguen³

¹formerly: Research School of Earth Sciences,

The Australian National University, Canberra, ACT 0200 AUSTRALIA

²currently: Discipline of Oceanography, School of Physical, Environmental and Mathematical Sciences,
University of New South Wales at ADFA, Canberra, ACT 2600 AUSTRALIA

³Ecole Normale Supérieure, Paris, FRANCE

Abstract

An idealised model is used to investigate the effects of variable wind forcing on basin-scale wind-driven ocean circulation. The circulation displays a rapid poleward current along the western coast which separates to form a free jet. Parameters are chosen so that the jet has a periodic time-variation under steady wind forcing, and we investigate how this intrinsic periodicity can be disrupted by a periodic variation in the wind forcing.

We show that the intrinsic oscillation is a linear instability of the jet which has saturated at finite amplitude, and eddy shedding occurs when negative streamfunction anomalies arrive at the terminus of the jet. When the forcing is periodic, Rossby waves carry the flow adjustment westward across the basin and the arrival of maxima produces periodic variations in the strength of the jet. If the forcing variation is sufficiently large and has a period close to a rational multiple of the intrinsic period, it can drive the jet instability, resulting in eddy shedding which is locked onto a rational multiple of the forcing period (nonlinear resonance). With weaker variations the eddy-shedding period may remain independent of the forcing, yielding a quasiperiodic flow. Chaotic or partially locked states are also observed, with variability on timescales far exceeding either the natural or forcing periods.

Introduction

The large-scale horizontal flow of subtropical oceans takes the form of a recirculating gyre in each ocean basin. Gyre circulations are highly asymmetric: a slow equatorward wind-driven flow (Sverdrup drift) occupies most of each basin, and this fluid returns poleward in a much faster and narrower current along each western boundary. These western boundary currents (WBCs), such as the Gulf Stream and East Australian Current, are among the most energetic features of ocean circulation. WBCs are climatically important due to their heat transport, and their variability has been implicated in climate fluctuations.

Dynamical-systems studies of idealised WBCs [11, 6, 3, 9] have revealed periodic, quasiperiodic and chaotic behaviour under *steady* wind forcing, with variability on seasonal to decadal timescales. Thus WBC variations may result from ocean-only dynamics, but since these intrinsic timescales overlap with those of the atmospheric forcing (e.g. the annual cycle, and the North Atlantic Oscillation) it is likely that variable wind forcing also plays a role.

An unstable WBC under variable forcing can be regarded as a forced nonlinear oscillator, and we may expect some of the behaviour typical of a forced nonlinear pendulum [1, 4]. The frequency of a nonlinear oscillator depends on its amplitude, and can therefore be shifted to allow resonance with a mismatched forcing frequency. Nonlinear oscillators can also resonate with forcing at a rational multiple of their natural frequency, or display a chaotic or quasiperiodic response to variable forcing.

These nonlinear effects may explain the response of ENSO to the annual cycle [7]. We investigate the relevance of these processes to WBC variability using an idealised model of a gyre driven by wind with a periodic component. We model the horizontal flow using the barotropic vorticity equation

$$\frac{\partial Q}{\partial t} + J(\psi, Q) = W - \delta_s \zeta + \delta_M^3 \nabla^2 \zeta, \quad (1)$$

where ψ is the streamfunction for the horizontal velocity, $\zeta = \nabla^2 \psi$ is the relative vorticity, $Q = \delta_T^2 \zeta + y$ is the potential vorticity, y is the northward position, J is the Jacobian operator and $W(t) = -1 + A \sin(f_w t)$ is the forcing by a spatially uniform anticyclonic wind stress curl with a periodic perturbation of amplitude A and frequency f_w . y is scaled by the basin width L , ψ is scaled by Sverdrup transport $\psi_{Sv} = \tau / (\rho \beta H)$, and the time t is scaled by L^2 / ψ_{Sv} , where τ is the surface wind stress, ρ is the fluid density, β is the northward gradient of the planetary vorticity¹ and H is the depth. The flow is governed by three dimensionless parameters: $\delta_s = (\beta L H)^{-1} \sqrt{A_v f / 2}$ and $\delta_M = L^{-1} (A_H / \beta)^{1/3}$ control the strengths of bottom and lateral friction, respectively, and $\delta_I = \sqrt{\psi_{Sv} / \beta L^3}$ controls the importance of advection. A_v and A_H are the coefficients of vertical and horizontal turbulent diffusion and f is the Coriolis parameter.

Flow governed by equation (1) has been studied numerically and in the laboratory in a basin with a circular no-slip boundary under steady forcing ($A = 0$) [2, 5, 8], and has a Hopf bifurcation from steady flow to periodic eddy-shedding from the WBC jet at a critical δ_I depending on δ_s and δ_M . We fixed $\delta_s = 1.01 \times 10^{-2}$, $\delta_M = 8.67 \times 10^{-3}$ and $\delta_I = 2.78 \times 10^{-2}$, to give periodic flow (with “natural” frequency f_n) when $A = 0$, and surveyed the behaviour in the (f_w, A) parameter space with over 230 runs (see figure 1). We studied the perturbation problem by writing $\psi = \bar{\psi} + \psi'$, $Q = \bar{Q} + Q'$, $\zeta = \bar{\zeta} + \zeta'$, where the overbars denote the unstable steady state solution to (1) with $A = 0$ (obtained numerically by Sheremet’s method [10]), and the dashed quantities are the solution to the perturbation equation

$$\begin{aligned} \frac{\partial Q'}{\partial t} + J(\bar{\psi}, Q') + J(\psi', \bar{Q}) + J(\psi', Q') \\ = A \sin(f_w t) - \delta_s \zeta' + \delta_M^3 \nabla^2 \zeta'. \end{aligned} \quad (2)$$

This system was solved in polar coordinates using the finite-volume code described by [8]. The linear stability was also investigated, by neglecting the nonlinear term $J(\psi', Q')$.

Results and Discussion

Figure 2 shows the periodic eddy-shedding cycle under steady forcing. The slow southward interior flow is returned in a rapid WBC which separates from the boundary to form an unstable

¹ β is a weak function of y to match the laboratory experiments of [5]

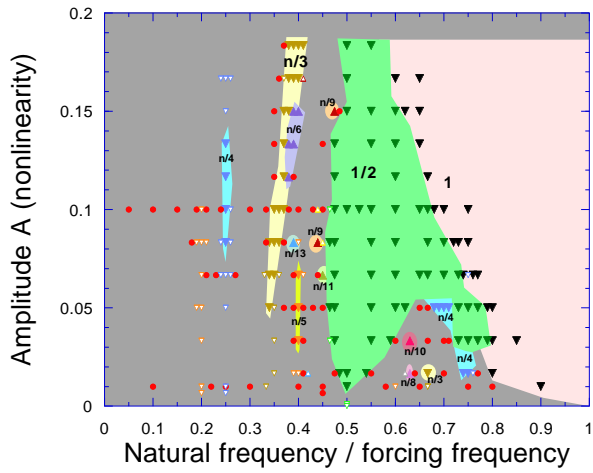
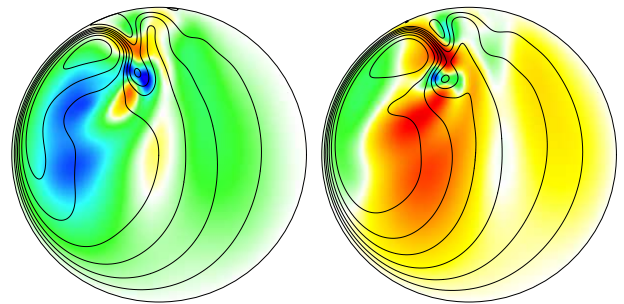
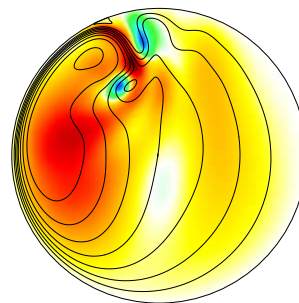


Figure 1: Locked regimes with various frequency ratios in the $(f_n/f_w, A)$ plane (the points outside the labelled regions yielded quasiperiodic or chaotic flow).



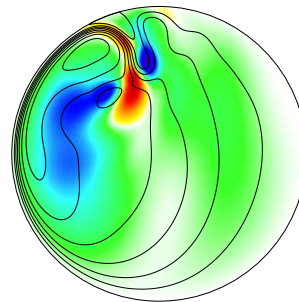
(a) 35 steps

(b) 175 steps



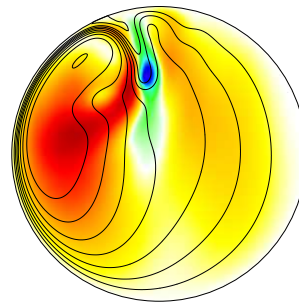
(c) 315 steps

(d) 455 steps



(e) 595 steps

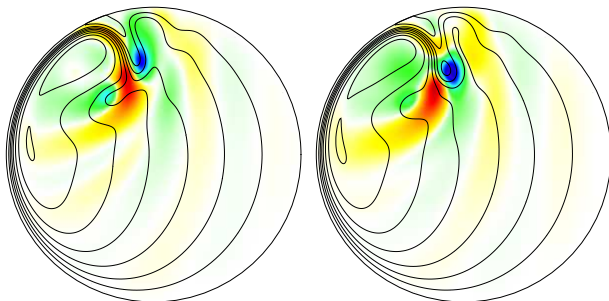
(f) 735 steps



(g) 875 steps

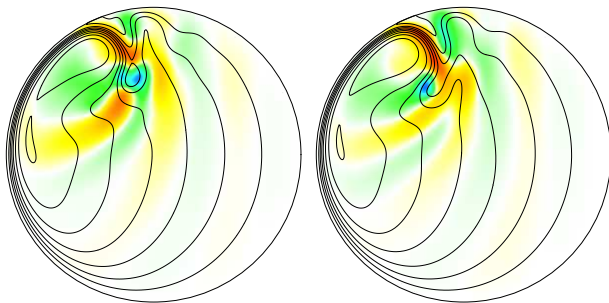
(h) 1015 steps

Figure 3: Eddy-shedding locked to double the forcing period, with $f_n/f_w = 0.52$, $A = 0.10$. The frames show two forcing periods, over which the flow completes one cycle. Streamlines indicate $\bar{\psi} + \psi'$ and colours indicate ψ' (blue, green $< 0 <$ yellow, red).



(a) 135 steps

(b) 405 steps



(c) 675 steps

(d) 945 steps

Figure 2: One eddy-shedding cycle under steady forcing. Streamlines indicate $\bar{\psi} + \psi'$ and colours indicate ψ' (blue, green $< 0 <$ yellow, red).

jet. The finite-amplitude perturbation in figure 2 closely resembles the most unstable linear eigenmode (not shown) but has an asymmetry between positive and negative perturbations. Eddy shedding corresponds to the arrival of negative streamfunction anomalies ψ' at the terminus of the jet. It appears that the instability growth saturates at finite amplitude due to energy loss by Rossby wave radiation (visible as the waves in the interior).

Figure 4(a) shows the flow's response to switching on the forcing perturbation (upper curve: W ; lower curve: perturbation kinetic energy K). The "natural" oscillation under steady forcing changes to a larger-amplitude, higher-frequency oscillation locked to $f_w = 1.35f_n$. This locking is evident in the plot of K vs. W (figure 4(b)), and has also been observed in a laboratory realisation of this system. Physically, the eddy-shedding is locked to f_w via forced fluctuations of the WBC mediated by Rossby waves, whose transit time across the basin produces a lagged response.

Locking at a wide variety of other rational frequency ratios was also observed; various locking ratios occur in complicated interleaved regimes in the $(f_n/f_w, A)$ plane (figure 1), reminiscent of "Arnol'd tongues" which occur with a forced nonlinear pendulum [1, 4]. Increasing the driving amplitude A increases the nonlinearity of the flow perturbation and allows locking to occur with a larger mismatch between f_w and f_n .

Figure 5 shows an example of eddy-shedding locked to $f_w/2 = 0.89f_n$ (the power spectrum in figure 5(c) shows the shift in the fundamental frequency from its (dashed) natural value). Figure 3 shows how westward-propagating Rossby waves mediate this locking by driving WBC perturbations which trigger eddy shedding. Locking may be absent when A is small and the mismatch large (f_n/f_w far from a simple rational), giving a quasiperiodic response (having a line spectrum with two incommensurate fundamental frequencies) as in figure 6. In other cases chaos was observed: figure 7 shows a response with partial locking onto $f_w/5 \approx f_n/4$, but unpredictable variations and broad-band noise in the spectrum. Note the large amount of power at frequencies well below both f_w and f_n .

Conclusions

Despite the high dimensionality of this fluid system, the nonlinear response of an unstable WBC to variable forcing shows a remarkable concurrence with low-dimensional driven pendulum theory. Locked "Arnol'd tongues" are observed, as well as chaotic states with low-frequency variability which is absent from the forcing or ocean in isolation. These results suggest that these nonlinear effects could contribute to low-frequency western boundary current variability.

References

- [1] Bak, P., Bohr, T. and Jensen, M. H., Mode-locking and the transition to chaos in dissipative systems, *Physica Scripta*, **T9**, 1985, 50–58.
- [2] Beardsley, R. C., A laboratory model of the wind-driven ocean circulation, *J. Fluid Mech.*, **38**, 1969, 255–271.
- [3] Dijkstra, H. A. and Katsman, C. A., Temporal variability of the wind-driven quasi-geostrophic double gyre ocean circulation: Basic bifurcation diagrams, *Geophys. Astrophys. Fluid Dyn.*, **85**, 1997, 195–232.
- [4] Glazier, J. A. and Libchaber, A., Quasi-periodicity and dynamical systems: an experimentalist's view, *IEEE Trans. Circuits and Systems*, **35**, 1988, 790–809.
- [5] Griffiths, R. W. and Kiss, A. E., Flow regimes in a wide 'sliced-cylinder' model of homogeneous β -plane circulation, *J. Fluid Mech.*, **399**, 1999, 205–236.
- [6] Jiang, S., Jin, F.-F. and Ghil, M., Multiple equilibria, periodic, and aperiodic solutions in a wind-driven, double-gyre, shallow-water model, *J. Phys. Oceanogr.*, **25**, 1995, 764–786.
- [7] Jin, F. F., Neelin, J. D. and Ghil, M., El Niño/Southern Oscillation and the annual cycle: Subharmonic frequency-locking and aperiodicity, *Physica D*, **98**, 1996, 442–465.
- [8] Kiss, A. E., Potential vorticity "crises", adverse pressure gradients, and western boundary current separation, *J. Mar. Res.*, **60**, 2002, 779–803.
- [9] Primeau, F. W., Multiple equilibria of a double-gyre ocean model with super-slip boundary conditions, *J. Phys. Oceanogr.*, **28**, 1998, 2130–2147.
- [10] Sheremet, V. A., A method of finding unstable steady solutions by forward time integration: relaxation to a running mean, *Ocean Modelling*, **5**, 2002, 77–89.
- [11] Speich, S., Dijkstra, H. A. and Ghil, M., Successive bifurcations in a shallow-water model applied to the wind-driven ocean circulation, *Nonlin. Process. Geophys.*, **2**, 1995, 241–268.

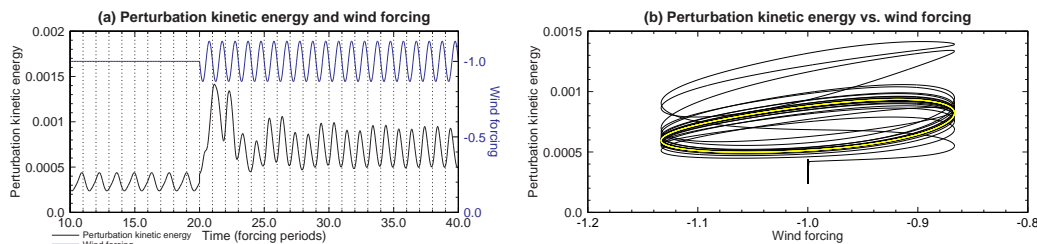


Figure 4: Locking to forcing frequency: $f_n/f_w = 0.74$, $A = 0.133$. The final attractor in (b) is shown in yellow.

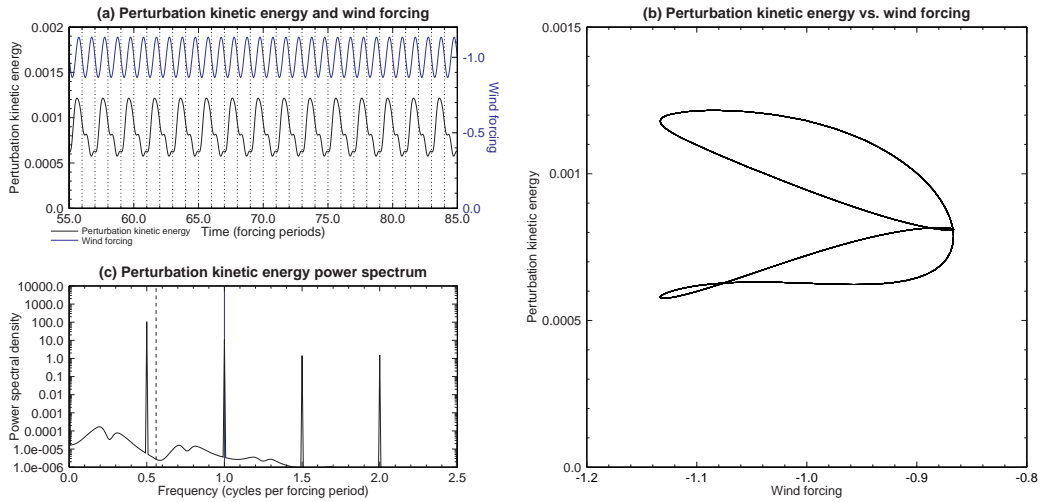


Figure 5: Locking to 1/2 forcing frequency: $f_n/f_w = 0.56$, $A = 0.133$

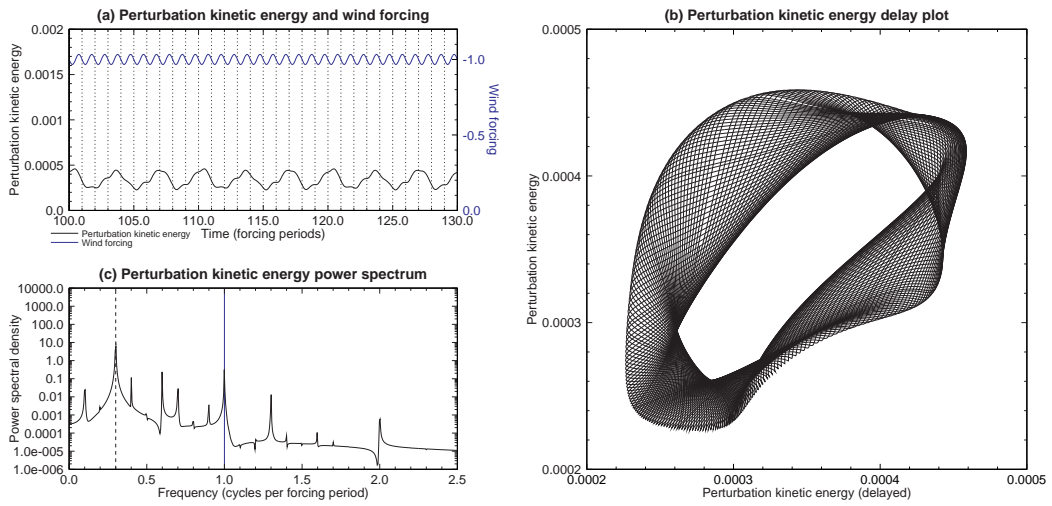


Figure 6: Quasiperiodic state: $f_n/f_w = 0.30$, $A = 0.0333$

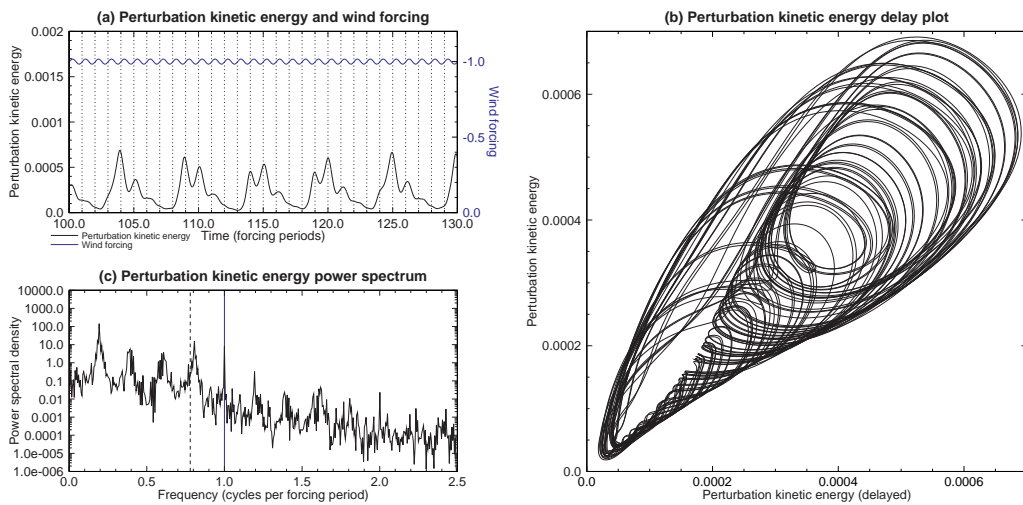


Figure 7: Chaotic state: $f_n/f_w = 0.78$, $A = 0.0167$